Electronic Supplementary Material (ESI) for Materials Horizons.
This journal is © The Royal Society of Chemistry 2023

Supporting Information

Dual-Functional Thermal Management Textiles for Dynamic Temperature Regulation Based on Ultra-Stretchable Spiral Conductive Composite Yarn with 500%-Strain Thermal Stability and Durability

Wei Chen,[a,b] Xiaoxiao Wei,[a,b] Wei Liu,[c] Fujun Xu*[a,b]

[a] Shanghai Frontier Science Research Center for Modern Textiles, Donghua University, Shanghai 201620, P. R. China

[b] Key Laboratory of Textile Science & Technology, Ministry of Education, College of Textiles, Donghua University, Shanghai 201620, P. R. China

[c] School of Fashion Technology, Shanghai University of Engineering Science, Shanghai, 201620, P. R. China

[*] Corresponding Author.

Email: fjxu@dhu.edu.cn

Table S1. Parameters and performance of typical stretchable heating materials.

Material	Structure	Process	Dimension (cm × cm)	Stretchability	$\Delta R/R_0$	Voltage (V)	Temp. (°C)	Tensile strain	$\Delta T/T_0$	Ref.
MWCNT nanopaper/PDMS	Composites	Ultrasonication treatment	2 × 0.5	Stable to 150% Unstable to 200%	132% 479%	15	180	5%	10%	1
CNT film/PDMS	Composites	Prestretching + coating	2 × 0.5	Stable up to 40% Unstable up to 110%	0.02% 40%	15	150	30%	6.60%	2
CNTY/PDMS/PU yarn	Fabric	Wrapping + weaving	5 × 2	Stable up to 50% Unstable up to 180%	5% 90%	2	47	50%	5%	3
CNT fiber	Yarn	Twisting CNT ribbons	2 cm length	Stable up to 40% Unstable up to 150%	26% 41%	4	100	140%	70%	4
Ag-NW/PDMS	composites	Coating	3 × 2.5	Stable up to 55% Unstable up to 200%	10% 600%	3	80	50%	27.00%	5
CNT/Cotton/Spandex	Yarn Textile	Twisting and Spinning Knitted Fabric	4 × 2	Stable up to 50% Unstable up to 400%	110% 200%	10	105	5%	2%	6
Graphene fiber	yarn	Twisted ribbon	6 cm length	Unstable up to 40%	150%	4	290	33%	81.84%	7
Ag-NW/PI film/Textile	Composites	Laser Cutting-Kirigami pattern	1.5 × 1.5	100% uniaxial and 50% biaxial	0.25%	0.125A	140	100% uniaxial 50% biaxial	0.10%	8
CuxS/PET fabric	Composites	Coating	3 × 1.5			2	172	50%	15.50%	9
GNSs/SBR	Composites	Scraping layer by layer		Stable up to 50% Unstable up to 100%	1% 26%	8	165	50% 100%	4.5% 27.3%	10
PPy/PU fiber/PET fiber	Textile	Coating +Weaving	4 × 2	Stable up to 50% Unstable up to 200%	3.5% 200%	7	80	100%	20%	11
Cu/nanocellulose paper	Composites	Printing + Cuting with Kirigami pattern	2.5 × 2.5	Stable up to 300%		0.15	50	300%	26.50%	12
Ag NP/PDMS substrate	Composites	Prestretching + thermal evaporation deposition	3 × 3	Stable up to 60%		3.8	60	60%	23.80%	13
Cu NW/PUA	Composites	Laster cutting + vaccum transfer	1 × 1	Stable up to 50% Unstable up to 125%	10% 200%	4	80	50%	0.10%	14
Ag NW/TPU	Composites	Laster ablation	11.6 ×6	Stable up to 60% Unstable up to 100%	10% 200%	1.5	50	50%	8%	15
Rgo/PEDOT:PSS/Cotton fabric	Textile	Coating	2 × 1			15	30.5	60%	20%	16
PHEA ionogels	Ionogel	Chemical polymerization + crosslinking	3 × 1	Stable up to 450%	25%	150	175	300%	42.90%	17
Cu NW/Chitosan/PDMS Substrate	Composites	Prestretching + coating	1 × 0.5	Stable up to 175% Unstable up to 200%	13% 300%	7.5	110	175%	25%	18
MWCNT/WPU/DTY	Yarn	Coating + Annealing + Coiling	1 cm length	Stable up to 500% Unstable up to 800%	8%	5	130	300% 400% 500%	3.90% 6.45% 8.40%	This work

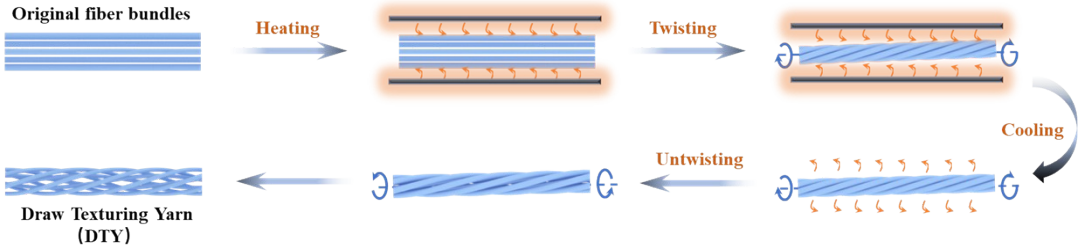

Figure S1. The preparation process of draw texturing yarn (DTY).

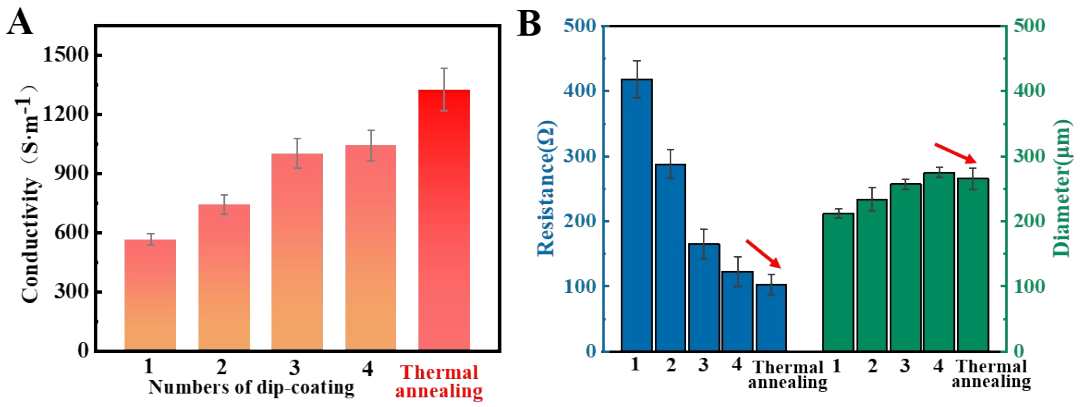

Figure S2. (A) Electrical conductivity of coated yarns with different dip-coating cycles and thermal annealing treatment. (B) The resistance and diameters of coated yarns with different dip-coating cycles and thermal annealing treatment.

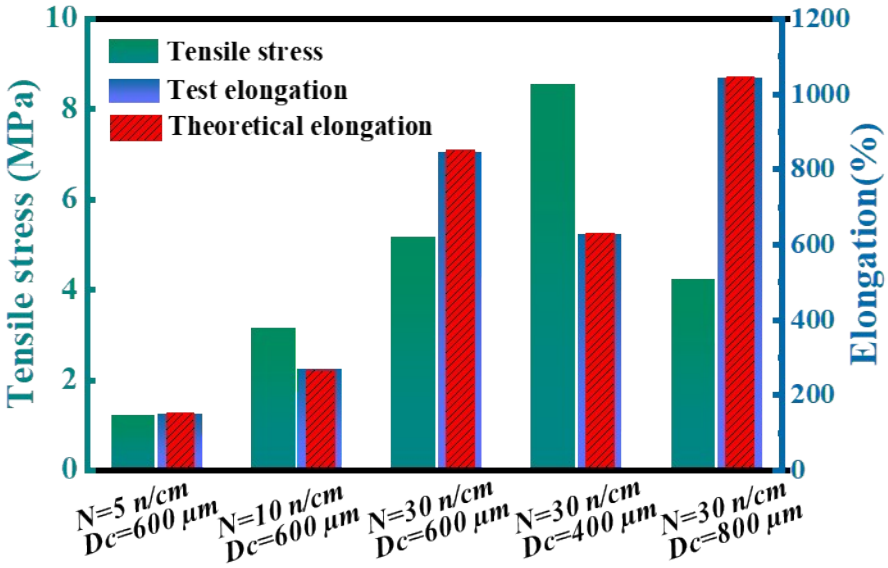

Figure S3. Tensile stress, theoretical elongation, and test elongation of SCCY with different structural parameters.

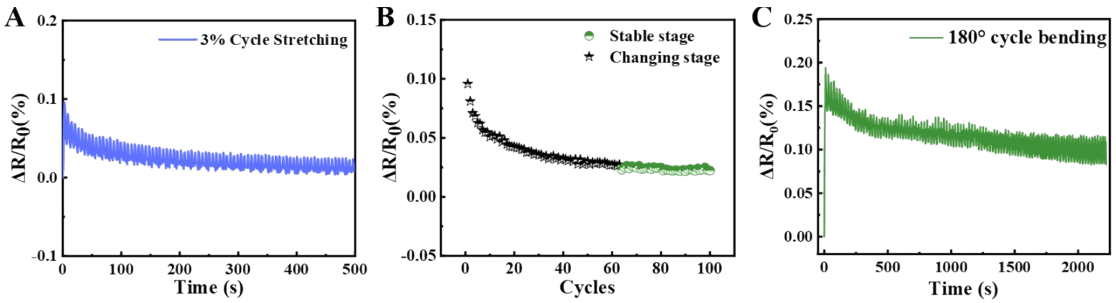

Figure S4. The relative resistance changes of T-CWCY under (A) and (B) 3% cycle stretching, and (C) 180° cycle bending.

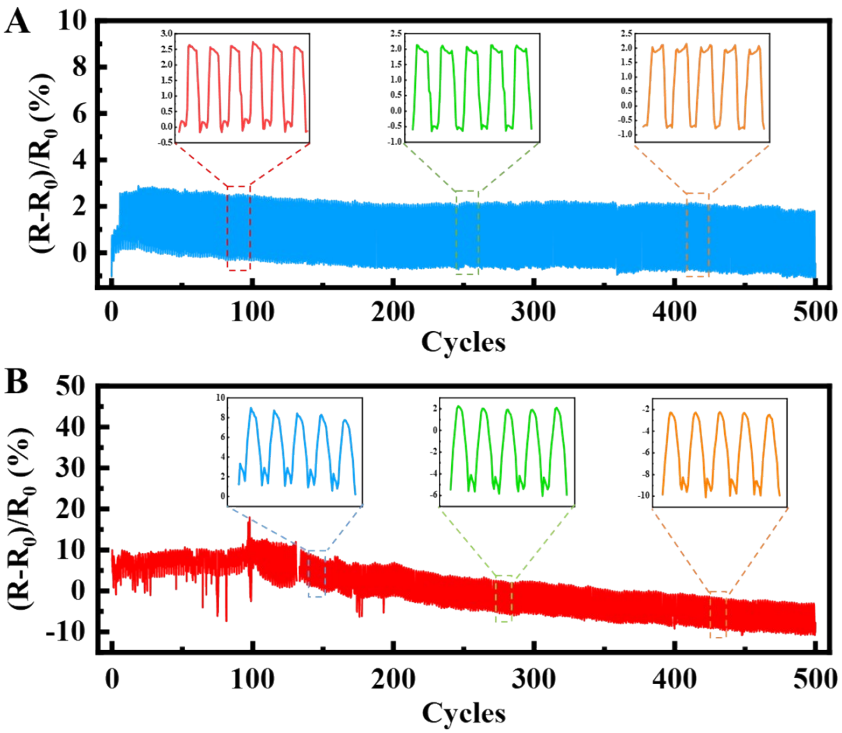

Figure S5. The relative resistance changes of SCCY under (A) 50% and (B) 100% cyclic stretching.

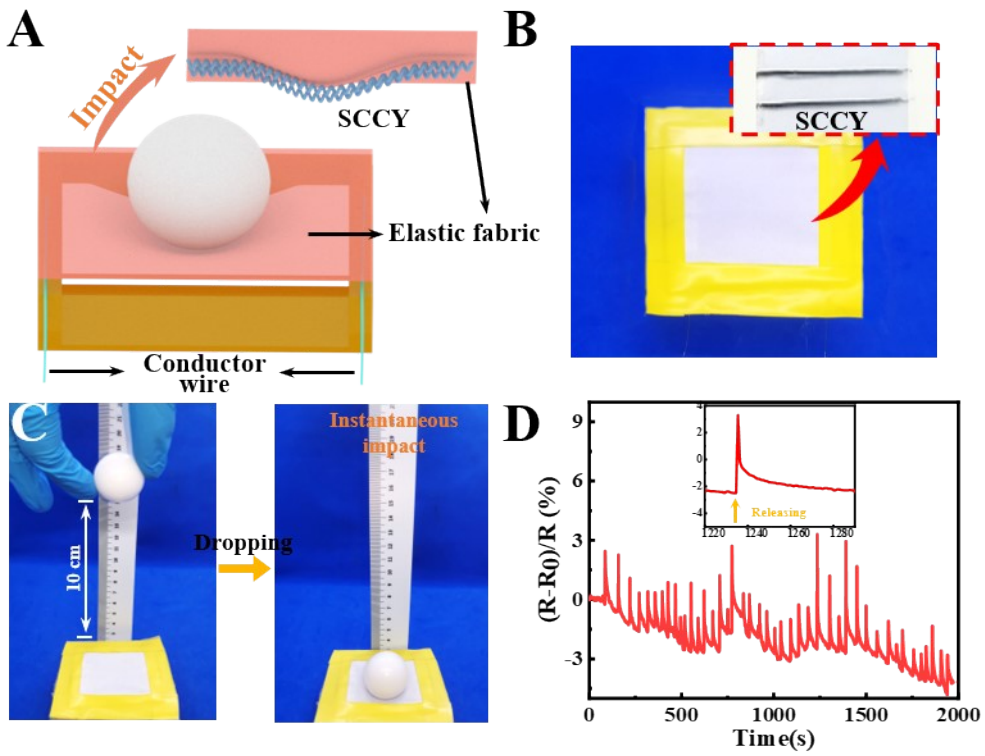

Figure S6. (A) Schematic illustration and (B) optical image of the impact electrical stability test of SCCY, in which SCCY is embedded on a suspended elastic fabric. (C) Photograph of the impact process on SCCY embedded in elastic fabric. (D) The resistance variations of SCCY under continuous impact test.

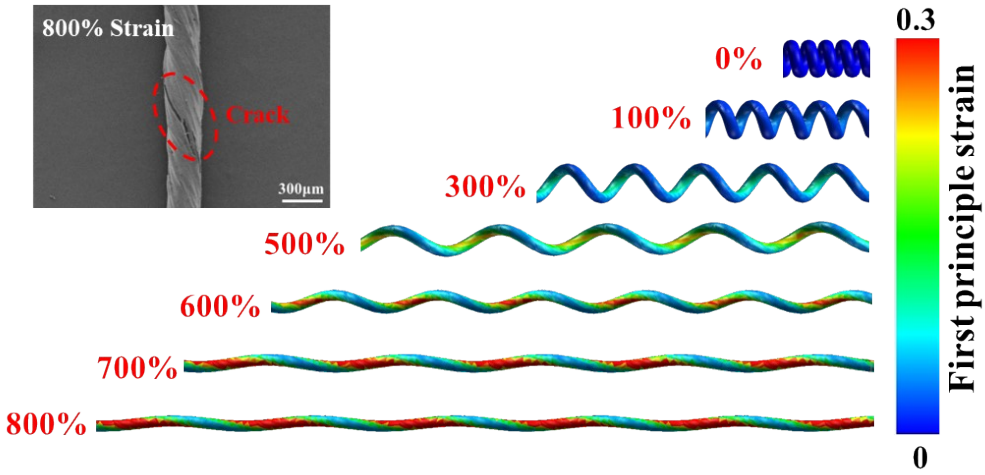

Figure S7. Distributions of the first principal strain in uniaxial tensile FEM models of SCCY from 0% to 800% (Insets represent the surface SEM image of SCCY under 800% strain).

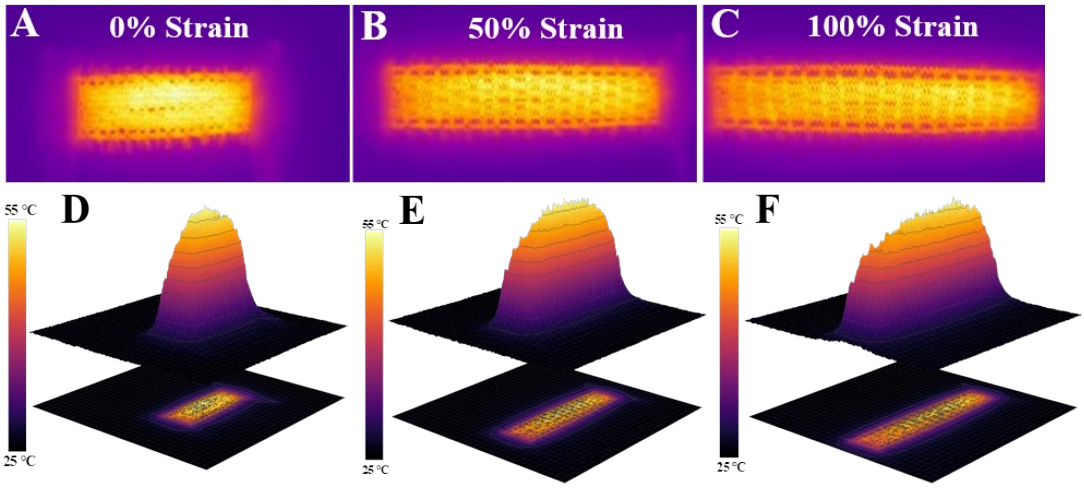

Figure S8. Infrared images and temperature distribution of stretchable electrothermal fabric at (A) static, (B) 50% strain, and (C) 100% strain.

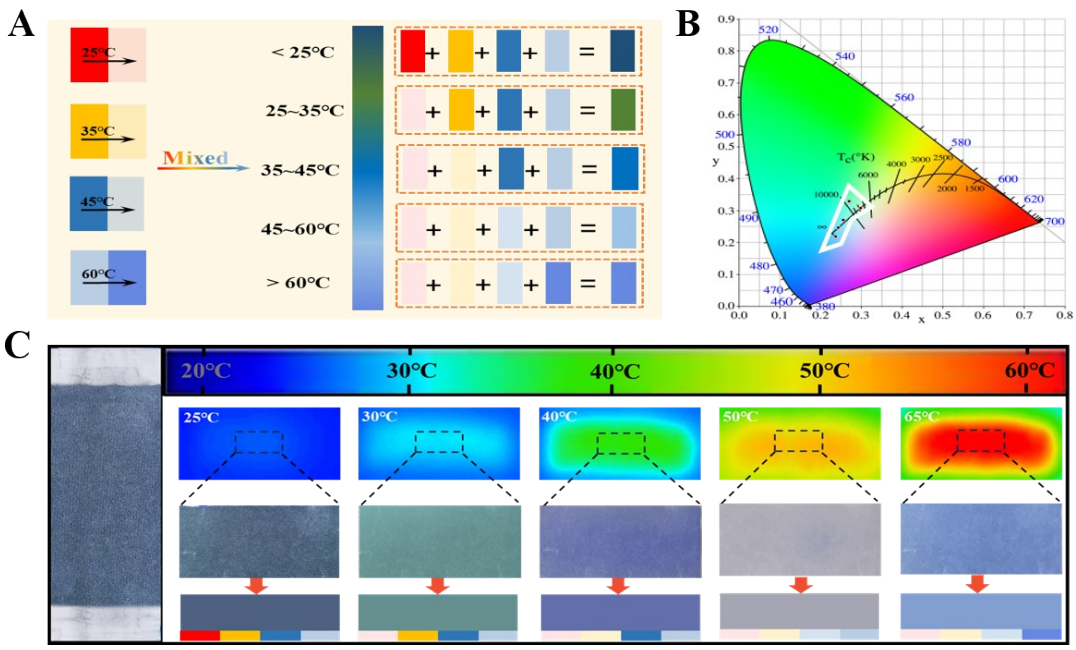

Figure S9. (A) Multilevel discoloration theory renderings. (B) CIE 1931 chromaticity diagram of color change of multilevel thermochromic ink. (C) Optical and infrared images of multilevel thermochromic textile under different temperature.

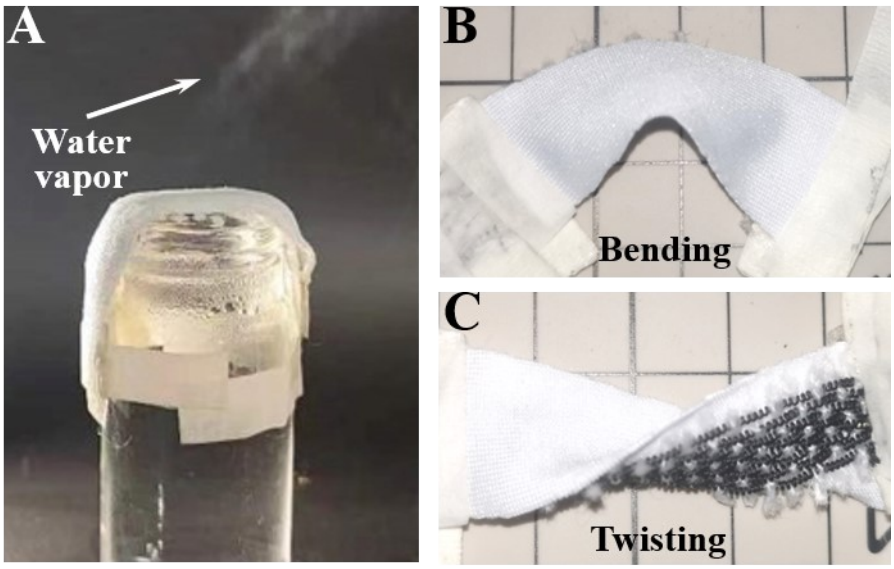

Figure S10. (A) The air permeability of the STMT. The excellent flexibility of STMT in (B) bending and (C) twisting conditions.

REFERENCES

1. J. Y. Sun, J. Zhuang, J. F. Shi, S. Kormakov, Y. Liu, Z. G. Yang and D. M. Wu, *J. Mater. Sci.*, 2019, **54**, 8436-8449.
2. F. J. Xu, M. A. Aouraghe, X. Xie, L. G. Zheng, K. Zhang and K. K. Fu, *Compos Part a-Appl S*, 2021, **147**.
3. J. H. Wu, Z. Y. Wang, W. Liu, L. H. Wang and F. J. Xu, *ACS Appl. Mater. Interfaces*, 2019, **11**, 44735-44741.
4. P. Liu, Y. M. Li, Y. F. Xu, L. K. Bao, L. Wang, J. Pan, Z. T. Zhang, X. M. Sun and H. S. Peng, *Small*, 2018, **14**.
5. D. Y. Han, Y. X. Li, X. Jiang, W. Y. Zhao, F. C. Wang, W. Lan, E. Q. Xie and W. H. Han, *Compos Sci Technol*, 2018, **168**, 460-466.
6. G. M. Cai, M. Y. Yang, J. J. Pan, D. S. Cheng, Z. G. Xia, X. Wang and B. Tang, *ACS Appl. Mater. Interfaces*, 2018, **10**, 32726-32735.
7. R. Wang, Z. Xu, J. H. Zhuang, Z. Liu, L. Peng, Z. Li, Y. J. Liu, W. W. Gao and C. Gao, *Adv Electron Mater*, 2017, **3**.
8. S. Wu, Z. Cui, G. L. Baker, S. Mahendran, Z. Y. Xie and Y. Zhu, *ACS Appl. Mater. Interfaces*, 2021, **13**, 59085-59091.
9. Q. Zhang, D. Liu, W. Pan, H. Y. Pei, K. L. Wang, S. A. Xu, Y. L. Liu and S. K. Cao, *J. Colloid Interface Sci.*, 2022, **624**, 564-578.
10. F. Wang, W. Wang, X. T. Mu and J. Mao, *Chem. Eng. J.*, 2020, **395**.
11. Y. M. Li, M. Q. Shan, J. M. Peng, L. Z. Lan, L. Q. Wei, L. M. Guo, F. J. Wang, Z. Zhang, L. Wang and J. F. Mao, *Appl. Surf. Sci.*, 2023, **610**.
12. Z. Li, A. Islam, M. Di Luigi, Y. L. Huang and S. Q. Ren, *Appl Mater Today*, 2023, **31**.
13. A. Hua, Z. F. Mai, B. Y. Wu, Z. C. Ji, M. Fu, Y. G. Hu and S. Y. Huang, *Mater Today Phys*, 2022, **26**.
14. D. Kim, J. Bang, W. Lee, I. Ha, J. Lee, H. Eom, M. Kim, J. Park, J. Choi, J. Kwon, S. Han, H. Park, D. Lee and S. H. Ko, *J Mater Chem A*, 2020, **8**, 8281-8291.
15. J. C. Wang, K. K. Zhang, J. Wang, M. H. Zhang, Y. L. Zhou, J. Cheng and D. S. Kong, *J Mater Chem C*, 2020, **8**, 9440-9448.

16. A. Ahmed, M. A. Jalil, M. M. Hossain, M. Moniruzzaman, B. Adak, M. T. Islam, M. S. Parvez and S. Mukhopadhyay, *J Mater Chem C*, 2020, **8**, 16204-16215.
17. L. M. Zhang, K. Jia, J. Wang, J. Y. Zhao, J. D. Tang and J. Hu, *Mater Horiz*, 2022, **9**, 1911-1920.
18. L. Zhao, S. H. Yu, J. J. Li, Z. C. Song, M. Y. Wu, X. Y. Wang and X. H. Wang, *J Mater Chem C*, 2021, **9**, 13886-13895.